

Population dynamics of the krill *Meganyctiphanes norvegica* (M. Sars, 1857) (Crustacea: Euphausiacea) in the Ligurian Sea (NW Mediterranean Sea). Size structure, growth and mortality modelling

J.Ph.Labat and J.Cuzin-Roudy

Laboratoire d'Océanographie Biochimique et Ecologie, Université P. et M. Curie (Paris 6) – INSU-CNRS, Observatoire Océanologique, 06230-Villefranche/mer, France

Abstract. The seasonal abundance, population structure and dynamics of the euphausiid *Meganyctiphanes norvegica* were studied from samples taken year round in the NW Mediterranean Sea. Length–frequency distributions were generally bimodal: the first mode was interpreted as the born-in-the-year cohort (0+) and the second as a combination of the older age classes (1+). To describe growth, a bilinear function provides the best fit. A growth rate of 0.052 mm day⁻¹ (1.56 mm month⁻¹) was calculated for the first part of the growth function and 0.0034 mm day⁻¹ for the second part. A negative exponential mortality function was fitted, giving a mortality rate of 0.0034 day⁻¹ (1.25 year⁻¹). A numerical simulation of the size structure of the Ligurian population was performed and the validity of the model was checked using a multifactorial analysis. The demographic characteristics of the Ligurian population were compared to those of other areas and were interpreted as a functional adaptation of *M.norvegica* to the southern part of the geographical distribution of the species.

Introduction

Euphausiids are important members of the pelagic community in most seas of the world. The northern krill, *Meganyctiphanes norvegica* (M. Sars, 1857), is the largest euphausiid species in the northern hemisphere. The species is present in the North Atlantic and adjacent seas (Mauchline and Fisher, 1969) and in the north-western part of the Mediterranean (Ruud, 1936; Franqueville, 1970; Boucher and Thiriot, 1972; Wiebe and D'Abramo, 1972). Northern krill are an important element of the pelagic food web as a trophic resource for fish, birds and whales (Pearcy *et al.*, 1979). In the north-western Mediterranean Sea, the species is frequently found in the stomach of high trophic level organisms: squid *Illex coindetti* by Sanchez (1982); red tunna, *Thunnus thynnus*, by Quynh (1978); and fin whales, *Balaenoptera physalus*, by several authors (Viale, 1985; Orsi Relini, 1992; Orsi Relini and Relini, 1993).

The population dynamics and production of *M.norvegica* have been studied in the North Atlantic and the adjacent seas (Einarsson, 1945; Mauchline, 1960; Matthews, 1973; Hollingshead and Corey, 1974; Jörgensen and Matthews, 1975; Berkes, 1976; Falk-Petersen and Hopkins, 1981; Lindley, 1982; Boysen and Bucholz, 1984; Mauchline, 1985; Astthorsson, 1990), but not in the Mediterranean, since the study of Ruud (1936).

Population dynamics of *M.norvegica* are affected directly and indirectly by multiple factors. For example, swarming behaviour, diel vertical migrations, seasonal reproduction and recruitment are all influenced by environmental factors acting at different scales (e.g. primary production, biotic parameters, fronts and gyres). The Ligurian front is a zone of enhanced productivity characterized by an

important spatio-temporal variability (Sournia *et al.*, 1990). The present investigation was based on a series of seasonal samples collected in the Ligurian Sea during successive years. The aim was to follow the changes in the population at the yearly scale despite a consistent local variability, and to develop and use the demographic functions to simulate a theoretical annual population cycle.

Method

Sampling

Samples were mainly collected on a seasonal basis over two successive years (1990 and 1991) in the Ligurian Sea. Fifty-eight samples were taken between 23 July 1990 and 6 November 1991, and three additional samples in January and February 1993.

The sampling area was situated between 6 and 12 nautical miles from Cap Ferrat (43°39'N, 7°22'E and 43°29'N, 7°37'E; Figure 1). Samples were acquired using I-KMT (Isaacs and Kidd, 1953) with a cod end of mesh size 5 mm and an ORI net (Omori, 1965) with a mesh size of 600 µm. The nets were towed obliquely for 30 and 20 min, respectively. Speed was between 2.0 and 2.5 knots, using the vessels RV 'Professor Georges Petit' or RV 'Korotneff'. The bottom depth in the area was 1000–2000 m. As *M.norvegica* performs diel vertical migrations, trawls were carried out from an approximate depth of 100 m to the surface at night, and from 700 m during the daytime (Quynh, 1978)

Sample treatment

The samples were preserved on board in 10% buffered formalin. *Meganyctiphanes norvegica* specimens were sorted and transferred to 70% ethanol with

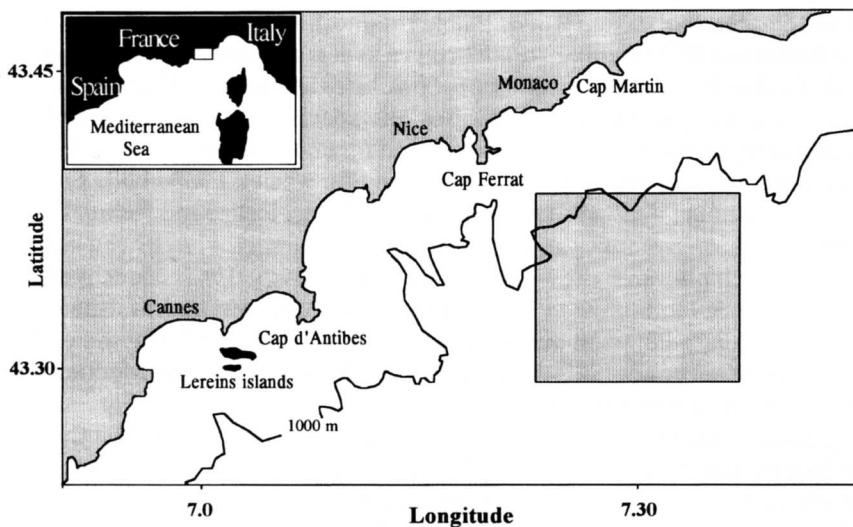


Fig. 1. Map of the sampling zone of the Ligurian population of *M.norvegica*.

1% glycerol. Large krill samples were split using a Motoda box and size of individuals was measured on random subsamples. Krill were identified and separated into three groups following Cuzin-Roudy (1993): juvenile (no secondary sexual characters), adult male (with petasma and/or ampullae), adult female (with thelycum). The sex ratio was expressed as the percentage of males among the total number of adult krill.

Body measurements were taken from drawings made with a camera lucida, using a digitalizer table (SummaSketch II) linked to a Macintosh computer. The total body length (BL) was measured to the nearest 0.1 mm, from the anterior tip of the rostrum to the distal end of the telson. To facilitate comparisons with data from the literature, Table I presents the relationship fitted to carapace length (CL) and BL using model II linear regression (Sokal and Rohlf, 1981).

Numerical methods

Length–frequency distributions and cohort separations. The estimation of demographic parameters in seasonally reproducing populations involves the discrimination of modes in length–frequency distributions, interpreted as age groups.

Graphic and numerical procedures (Harding, 1949; Hasselblad, 1966; Grant *et al.*, 1987) were used to separate overlapping normally distributed components and estimate means, standard deviations and relative frequencies of the different modes. The rough estimations given by the graphical methods were used as initial values for the numerical methods. We used the NormSep program (Abramson, 1971) in a version implemented in an MS-Dos computer and SYSTAT software to compute parameters of non-linear functions.

Estimation of the demographic functions. The principal demographic functions were studied by cohort analysis using length–frequency distributions established for the successive seasonal samples. The two demographic functions: (i) growth and (ii) mortality, were fitted from the parameters calculated for the different cohorts of the successive seasonal samples.

(i) *Growth:* two kinds of relationship were used. The commonly used von Bertalanffy function is written as:

$$BL_t = BL_{inf} - (BL_{inf} - BL_{min})\exp^{-K(t - T_0)}$$

where BL_t is BL at time t , BL_{inf} is the maximal theoretical size, BL_{min} is the minimal size, K is the Brody coefficient and T_0 is the time at the minimal size.

Table I. Linear regression (model 2) between carapace length (CL) and body length (BL) of the Ligurian krill, *M.norvegica*

	<i>N</i>	<i>R</i>	Regression
Juvenile	223	0.983	CL = 0.256 BL + 0.115
Male	388	0.962	CL = 0.247 BL + 0.282
Female	342	0.924	CL = 0.298 BL - 0.904

N, number of krill; *R*, correlation coefficient.

A bilinear function gave a better fit to the data:

$$BL_t = a_1t + b_1 \text{ for } t < c$$

$$BL_t = a_2t + b_2 \text{ for } t > c$$

where c is the time where the growth model changes.

(ii) *Mortality*: the mortality rate can be estimated when a relationship between the strengths of age classes can be estimated, with the following restrictive assumptions (Brey, 1986): stationarity in time (no year-to-year changes, no variability in mortality rates), and random distribution of age groups in the samples.

The commonly used mortality function is written as:

$$N_{t_2} = N_{t_1} \cdot \exp^{-m \cdot (t_2 - t_1)}$$

where N_t is the number at time t and m is the mortality coefficient.

If the second mode corresponds to a superimposition of several older cohorts, the strength of the second mode can be rewritten as the sum of several cohort strengths of successive years, as shown below.

$$N_{c2} = N_{c1} \cdot \exp(-dt \cdot m) + N_{c1} \cdot \exp(-2 \cdot dt \cdot m) + N_{c1} \cdot \exp(-3 \cdot dt \cdot m) + \dots$$

where N_{c1} and N_{c2} are the strengths of the two modes, dt is an interval of 1 year and m is the annual mortality coefficient.

Simulation of the size structure of a theoretical population. A simulation procedure was used to generate the size structure of a theoretical population during successive annual cycles, using the mortality and growth functions and a time interval of 1 month. The hypothesis was that, at a given time, the size structure is the sum of several normally distributed cohorts.

The mean BL for each cohort was computed from the growth function, the standard deviation from the relationship between the observed standard deviations and mean BL of the cohorts, and the strength values from the mortality function. An iterative procedure generates random individual BL values out of a normal distribution characterized by these parameters and strengths. Length–frequency distributions were built with the simulated BL at each time step.

Correspondence analysis. Correspondence analysis (CA) (Benzecri, 1973) was used here to analyse the annual variability of the population structure and to verify the similarity between the observed and the simulated patterns. CA is an ordination method which has been widely used in the analysis of ecological data (Gower, 1987) and especially to describe size structures (Badia and Do-Chi, 1976). Its aim is to describe the total inertia of a multidimensional set of data, in a sample of fewer dimensions (or axes) that is the best summary of the information contained in the data. Among the inertia methods, CA employs contingency tables and uses a χ^2 metric. Starting from the cloud of samples within the size classes space, and the

cloud of size classes in the samples space, this factorial analysis provides the best possible summary of the kinetics of the size structure of a population over time, in a new space of reduced dimensions. The position of a sample in the multivariate space is defined using all the size classes: closeness reflects similar abundance and distance reflects scarcity. Picard (1982) has shown that the topography in the 1–2 plane of cyclical biological data reflects not only the growth, but also the scatter of the observations between the classes of the length–frequency distribution.

CA allows a comparison of computed or simulated data with observed data (Badia and Do-Chi, 1976; Labat, 1991) and will be used to check the quality of the simulation of size structures: the evolution of observed and simulated size structures in the main factorial planes allows the quality of the method to be appreciated. CA was carried out with BIOMEKO software.

Statistical tests. The general agreement between the fitted functions and the data was checked by ANOVA (explained mean square over the unexplained mean square) (Sokal and Rohlf, 1981). For linear regression, a Durbin–Watson test (DW) was used to test the autocorrelation of the residuals (Wannacott and Wannacott, 1991); for a non-linear model, the one-sample runs test (Sokal and Rohlf, 1981) was used to test the randomness of the residuals. The Kolmogorov–Smirnov two-tailed test (Siegel and Castellan, 1988) was used to compare the cumulative frequencies of the size distributions; the binomial test to verify a sex ratio of 0.5.

In all these tests, the null hypothesis, H_0 , was rejected when the probability of the observed event (P_{obs}) was <0.05 .

Results

Analysis of the samples

Meganctiphanes norvegica was present in 51 out of the 61 samples, and 6944 krill were caught and counted. Forty-five samples with more than five individuals were used for the general size comparison (CA), 33 with more than five adults for sex ratio analysis, and 20 with sufficient numbers of animals for size structure analysis methods.

The total number of krill measured was 3894: 1499 females, 1411 males and 984 juveniles. The general sex ratio was not different from 0.5 (Binomial test $p = q = 0.5$, $n = 2910$, $z = 1.61$, $P_{\text{obs}} = 0.054$). Figure 2 shows the distribution of the sex ratio of 33 samples with more than five adult krill. For only 12 samples out of the 33, a binomial test showed that the hypothesis of equiprobability of occurrence for males and females did not hold at the 5% level.

The size distributions for females, males and juveniles, summed for all samples, are presented in Figure 3. The smallest observed size was BL = 7.5 mm, the largest BL = 37.5 mm. Adult males and females could be recognized from a BL size of 19 mm, but krill without secondary sexual characters were classified as juveniles up to BL = 26 mm. The size distributions for males and females did not differ significantly (Kolmogorov–Smirnov two-tailed test for 1499 males and 1411 females, $D_{\text{obs}} = 0.0476 < D_{0.05} = 0.0504$).

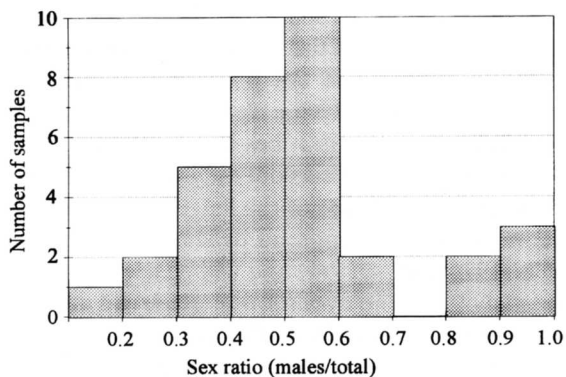


Fig. 2. Frequencies of the sex ratio in the 33 krill samples with more than five adult krill.

Modal analysis

Twenty samples were used to distinguish the modes and define the cohorts (with more than 50 individuals, one exception for the 6 November 1991 sample for which a numerical splitting method was not used, the parameters were computed directly from the individuals). Length–frequency distributions of males, females and juveniles are presented in Figure 4. A bimodal distribution was observed for most of the samples, except for the first months of the year (Figure 4s and t). The mode corresponding to the large size was present throughout the annual cycle. The first mode, corresponding to the small sizes, was interpreted as the born-in-the-year animals (0+), the second mode as krill older than 1 year. The first occurrence of juveniles was observed in a March sample (4 March 1991) (data not shown). Maximum recruitment was in April–May (Figure 4g and h) and a few small size krill (BL < 13 mm) were still found in July (Figure 4b and j). The (0+) cohort showed a rapid increase in size until January of the next year (Figure 4g–r). Table II gives the

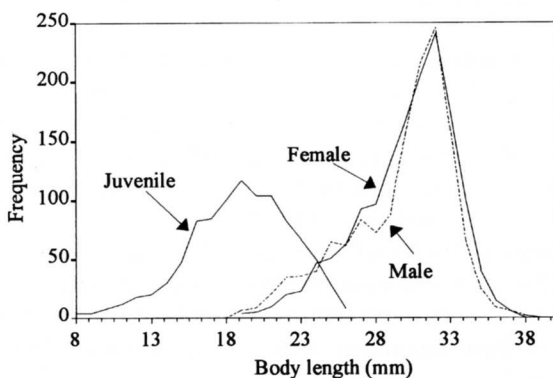


Fig. 3. Length–frequency distributions of juveniles, males and females cumulated for the 51 samples where *M.norvegica* was present. Frequencies of body length (BL) in 1 mm classes.

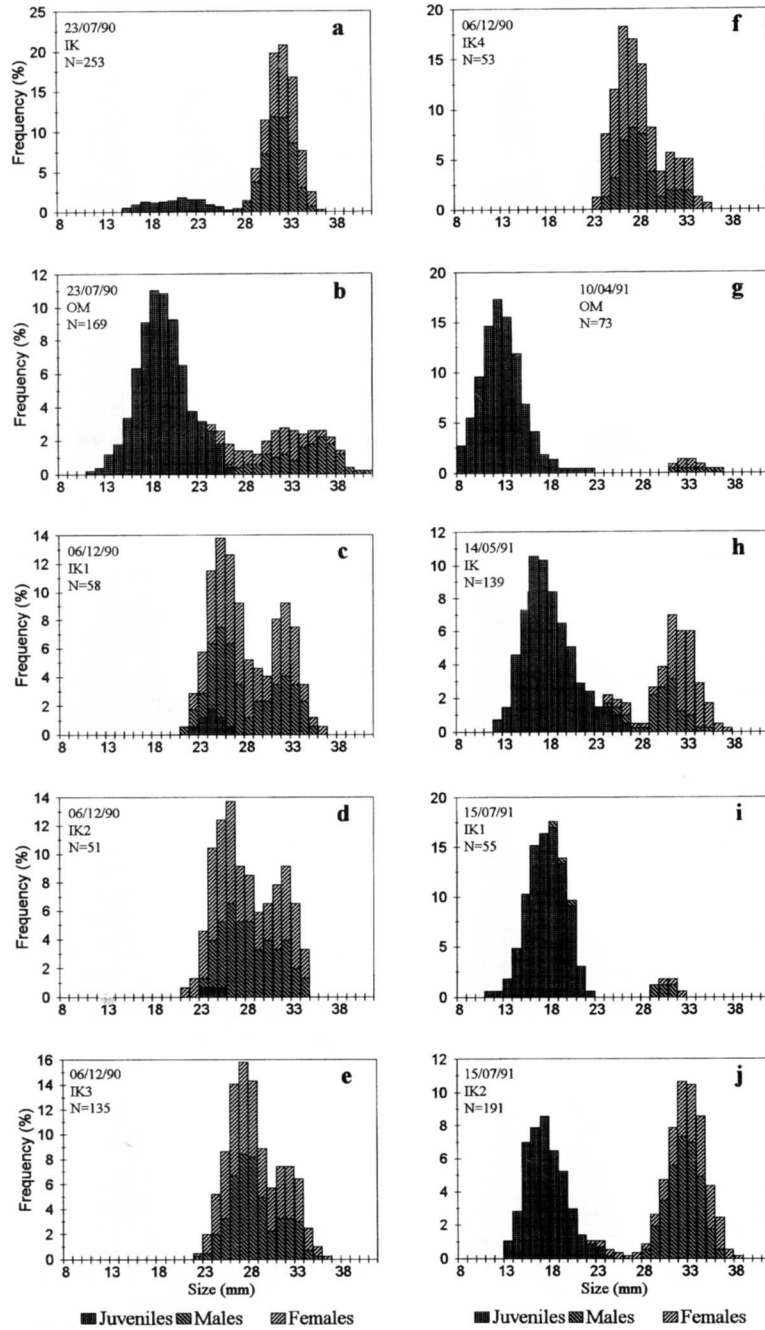
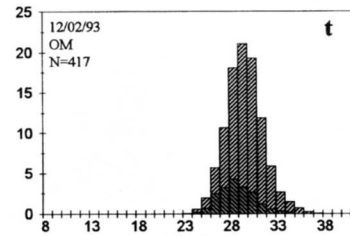
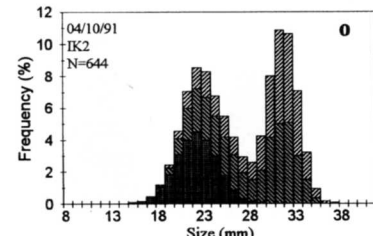
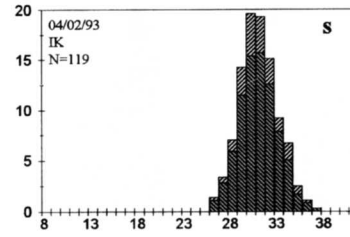
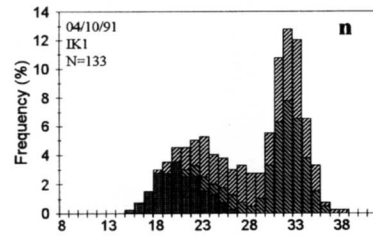
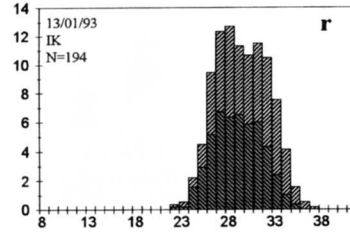
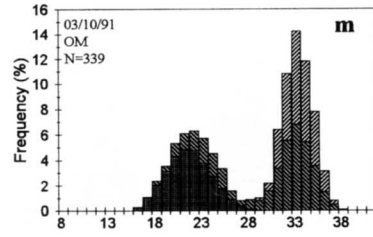
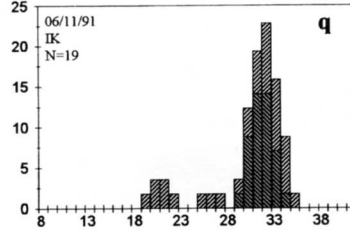
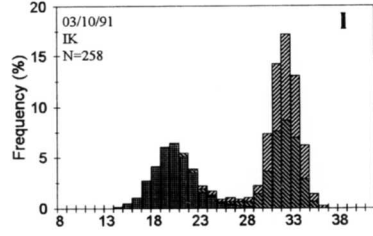
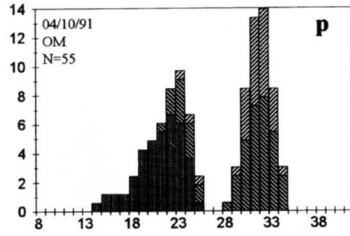
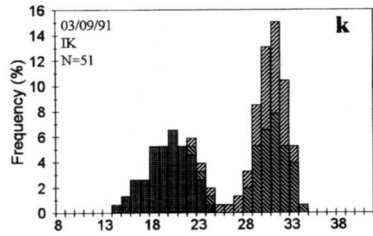


Fig. 4. Length–frequency histograms for the juvenile, male and female krill of the 20 samples used for cohort analysis. Relative frequencies (%) of body length size classes in 1 mm classes. (a–t) Samples from July 1990 to February 1993. Date, type of net (I-KMT = IK and ORI net = OM) and number of animals (N) are given. (Fig. 4. part ii overleaf)



■ Juveniles ▨ Males ▩ Females

■ Juveniles ▨ Males ▩ Females

Table II. Parameters of the bimodal length–frequency distributions of the samples

Sampling date	Mean		Standard deviation		%	
	Mode 1	Mode 2	Mode 1	Mode 2	Mode 1	Mode 2
23 July 1990	19.98	31.21	2.88	1.32	13.9	86.1
23 July 1990	18.43	31.96	2.72	–	72.1	27.9
6 December 1990	24.95	31.52	1.66	1.25	65.4	34.6
6 December 1990	25.40	31.18	1.79	1.14	67.2	32.8
6 December 1990	26.38	31.61	1.63	1.11	73.9	26.1
6 December 1990	26.13	31.49	1.60	1.22	81.1	18.9
10 April 1991	11.81	32.50	2.12	1.40	93.1	6.9
14 May 1991	17.49	31.33	3.10	1.64	68.7	31.3
15 July 1991	16.77	29.83	1.97	0.85	94.5	5.5
15 July 1991	16.81	31.90	2.21	1.85	46.1	53.9
3 September 1991	19.61	30.16	2.60	1.18	43.2	56.8
3 October 1991	20.03	31.40	2.68	1.15	37.9	62.1
3 October 1991	21.40	32.59	2.39	1.47	41.6	58.4
3 October 1991	22.23	31.74	3.38	1.45	46.8	53.2
3 October 1991	22.42	30.91	2.41	1.40	53.9	46.1
4 October 1991	20.81	30.97	2.39	1.05	49.2	50.8
6 November 1991	20.00	30.97	–	1.76	10.5	89.5
13 January 1993	26.77	31.04	1.55	1.60	52.4	47.6
4 February 1993	29.48	31.76	1.43	1.64	63.7	36.3
12 February 1993	28.70	33.38	1.56	1.03	96.3	3.7

parameters computed for the modes of the different samples. In Figure 5A, the mean BL of the modes was plotted against the sampling dates, illustrating the growth of the first cohort and the permanence of the second one.

Growth

From the kinetics of the mean size of the modes, we can estimate an average growth rate. In Figure 5B, mean body length of the mode was plotted against time.

A von Bertalanffy growth function was first used. The fitted equation was:

$$BL_t = 34.62 - (34.62 - 8) \cdot \exp^{-0.00371 \cdot (t - 64.6)} \text{ with } R^2 = 0.997$$

The overall fit of the model was satisfactory (ANOVA, $F = 3997.5$, ddl: 3.37, $P_{\text{obs}} < 0.001$), but the test of the residuals showed that they were non-random (runs test, for H_0 random distribution of residuals, $P_{\text{obs}} = 0.011$). We concluded that the model was not suitable for our data. The fitted equation is only given here to allow a comparison with the former studies on *M.norvegica*.

A better fit was obtained with a bilinear function, as shown in Figure 5B (ANOVA, $F = 4292.6$, ddl: 5.35, $P_{\text{obs}} < 0.001$; $R^2 = 0.998$; a run test on the residuals did not indicate a rejection of the H_0 random distribution of residuals, $P_{\text{obs}} = 0.43$). The calculated equations were:

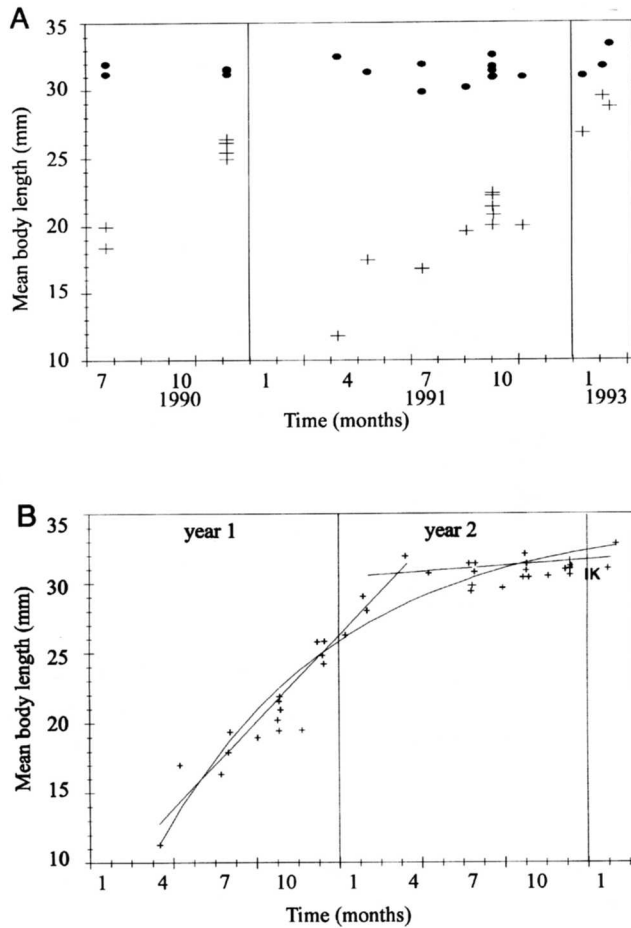


Fig. 5. (A) The mean body length (BL) of the cohorts plotted against the sampling dates. The 0+ cohort is labelled by crosses and the older one by filled circles. (B) Growth curves (von Bertalanffy and bilinear models) fitted to the cohort mean body length (BL), during two hypothetical successive years.

$$BL_t = 0.052t + 7.406 \text{ for } t < 466$$

$$BL_t = 0.0034t + 29.20 \text{ for } t > 466$$

Therefore, the bilinear growth function was used for the simulation of the size structure of the theoretical population.

Size scatter inside the modes

A negative relationship between standard deviations and mean BL of the different modes (Figure 6) indicated that small krill were more scattered than large adults ($R = -0.785$, for 38 pair values, $P_{\text{obs}} < 0.05$). A wide scatter of the size range in the 0+ cohort could be an effect of a long period of recruitment. A linear

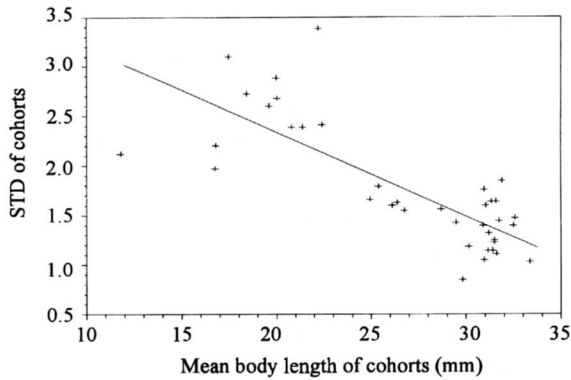


Fig. 6. Cohort scattering in relation to size. The standard deviations of the mean body length (BL) of the cohorts are plotted against the means and a linear regression is drawn.

regression was computed between the standard deviations of modes (STD) and their mean sizes (mean BL).

$$\text{STD} = -0.0842 \text{ BL} + 4.022$$

($R^2 = 0.616$, ANOVA: $F: 57.7$, $\text{ddl}: 1.36$, $P_{\text{obs}} < 0.001$; Durbin–Watson test, $D = 1.882$, $P_{\text{obs}} > 0.05$). This function was used to compute the standard deviation of the cohorts in the numerical simulation of the size structure of the theoretical population.

Mortality

To estimate a coefficient of mortality, we only used data from periods with no recruitment, when the cohorts were proximate but still distinct in size (samples of December, January and February; Figure 4). We assumed that the two size groups had the same behaviour and distribution during these periods. The average proportions of the two modes were, respectively, 71.4% for the first and 28.6% for the second. With the mortality model used, the second mode cannot be interpreted as a single age class, we postulated that it represented a combination of slow-growing older age classes. Under this condition, we obtained a solution where $m = 1.248 \text{ year}^{-1}$ (0.0034 day^{-1}), with 28.7% of a cohort reaching the age of 1 year, 8.2% 2 years and an average longevity close to 6.7 months.

Simulation of the size distribution of the theoretical population

Using the fitted functions obtained for growth, mortality and BL scattering, a size distribution of the theoretical population was generated over several successive annual cycles with a time step of 1 month. Figure 7 shows the simulated size structure over 3 years. This model illustrates the two growth phases with yearly recruitment occurring from March to July, a stable large size mode and in between classes rapidly increasing in size.

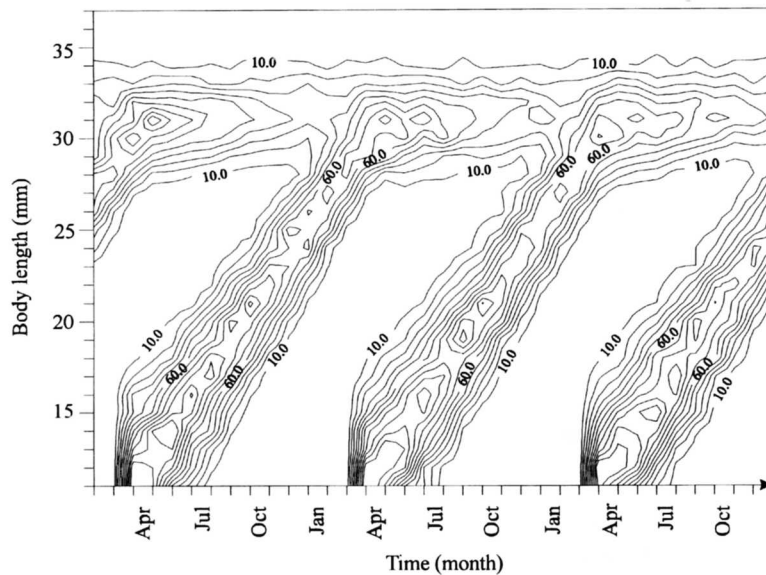


Fig. 7. Simulation of the size structure of a theoretical population during three successive years, in months. Isocontours are drawn for the abundance of size class frequencies (step of 10).

Correspondence analysis was used to describe the variation of the size structures with time. The CA data table contained the number of simulated animals per size class, for each time step. The observed values of size structure from 45 samples (with more than five individuals) were added to the analysis as supplementary data. Size classes below 14 mm and over 37 mm with weak strength were summed into the two extreme classes.

The projections of the simulated monthly size structures (I–XII) in the plane of factors 1 and 2 are represented in Figure 8A together with the contours of the observed samples of the same month. The projections of the size classes (mid-class BL values) are presented separately in Figure 8B. The plane 1–2 represents 76% of the inertia of the cloud, with 45.9 and 30.3% for the first and second axes, respectively. The other axes were considered negligible.

The projections in the 1–2 plane of the simulated monthly samples are organized in a circular pattern. The size classes showed a regular trajectory, with the smallest BL located on the periphery and the largest near the centre of the plane. These two figures, viewed in superimposition, reflect the variation of size over time. They should be interpreted as the result of (i) rapid growth for the small krill during the first year, from March to the following February (BL classes 11.5–28.5 mm), and (ii) slower growth of the large krill after the first year, resulting in an apparent stability of their size year round.

Good agreement of the kinetics between the simulated and the observed samples can be deduced from their topological proximities in the 1–2 plane. The simulated samples fall inside the contours of the observed samples of the corresponding month. The distance of a given month sample from the centre of the

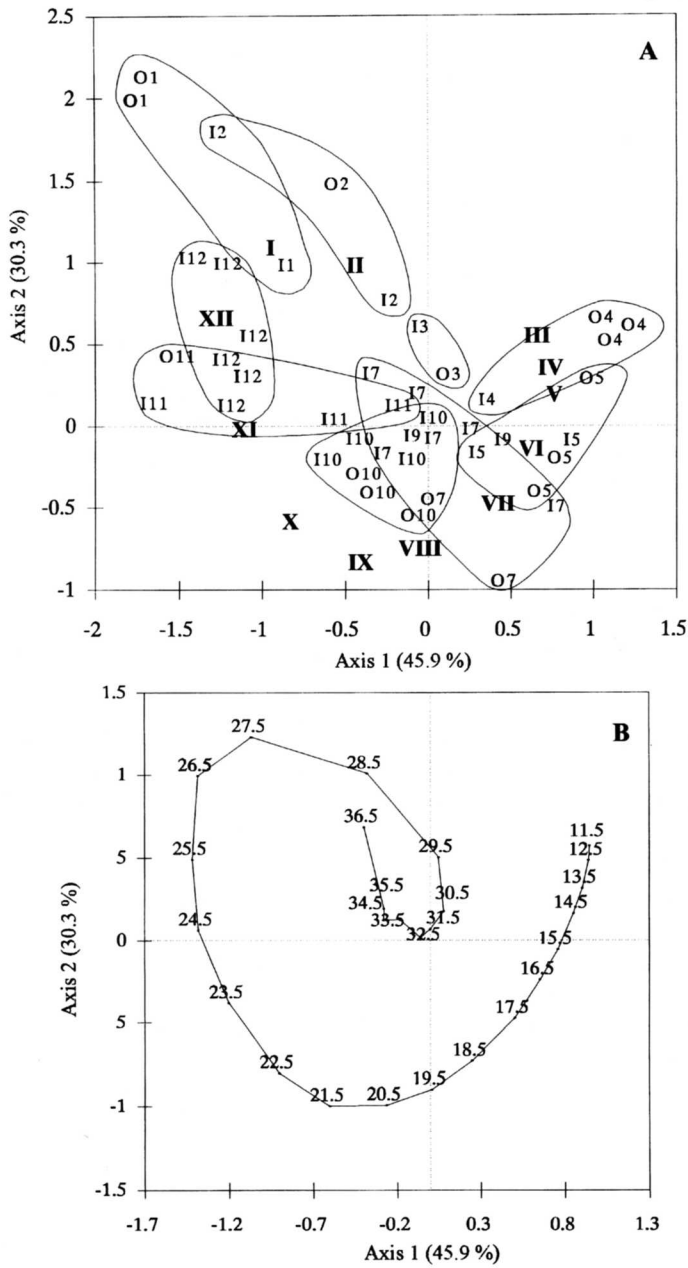


Fig. 8. Correspondence analysis of the observed and simulated size structures. Plane of the axes 1 and 2 (76% of the inertia). **(A)** Simulated monthly samples for 1 year are shown in Roman numerals (I–XII), observed monthly samples are labelled following the net type (O: ORI net; I: I-KMT) and the number of the actual month of sampling (e.g. I11 is a sample taken with an I-KMT in November). A contour is drawn around the observed samples of a given month. **(B)** Ordination of the body length classes (expressed in mm). The patterns for samples (A) and size classes (B) are presented separately for clarity, but should be superimposed for interpretation of the analysis (see the text).

plane depends on the presence of one or two modes and their relative importance. Samples with a predominant small size mode fall towards the periphery, and samples with only one or a predominant large size mode lie near the centre. This is also confirmed by the position of the samples obtained by ORI net and I-KMT, because the ORI net selects smaller krill than the I-KMT. ORI samples fall outside the I-KMT sample in the 1–2 plane, mostly from April to July when the size differences between the two modes were most pronounced.

Discussion

Population structure

Our samples of *M.norvegica* show considerable variation with regard to krill sex ratio and size structure, despite the restricted area of the Ligurian Sea where they were caught. The variability in time is linked with life cycle and seasonal reproduction. The origin of instantaneous variability (variability in space) might be found in the patchiness of the krill population in relation to swarming behaviour, well documented for other populations of *M.norvegica* (Sameoto, 1983; Falk-Petersen and Kristensen, 1985; Nicol, 1986). Another cause of variability could originate from hydrographic conditions of the sampling area close to the Ligurian front where *M.norvegica* is commonly present (Quynh, 1978; de Labigne 1985; Miquel and Labat, 1992). This zone shows a strong variability in its physicochemical structure at a small space scale (1–10 nautical miles) as well as time scale (1 day–1 week) (Boucher *et al.*, 1987; Ibanez and Boucher, 1987; Sournia *et al.*, 1990).

Variability in the sex ratio was large when considered at a short scale, but globally the sampled krill population displayed values not different from 0.5. The same explanation as above can apply to the variability between cohorts. Demographic differences between swarms have been described previously for populations of the North American east coast (Hollingshead and Corey, 1974; Nicol, 1986).

In the NW Atlantic, reproduction and recruitment of *M.norvegica* essentially take place during summer (Hollingshead and Corey, 1974; Berkes, 1976; Lindley, 1982) as off the coast of Norway and in the Baltic Sea (Matthews, 1973; Jörgensen and Matthews, 1975; Boysen and Buchholz, 1984). In other Atlantic populations, these phenomena seem to occur earlier: reproduction occurs in March/April/May and recruitment from May to summer (Lindley, 1982; Mauchline, 1985; Astthorsson, 1990). In the Ligurian population, recruitment was considered as occurring from March to June, in agreement with the observed reproductive period which has been shown to be from February to May (Cuzin-Roudy, 1993). These different timings for the reproductive season in different areas can be interpreted as life cycle strategies responding to various environmental conditions.

Growth

The growth pattern of the Ligurian population of *M.norvegica* is characterized by a rapid increase in body size during the first year. Growth then slows down, with the rate decreasing by more than 10. This drastic change in growth rate corresponds in time to the reproductive effort. Alternation between somatic and

gonadal growth is probable, as somatic growth slows when the gonads start actively to develop sexual products. In the same population, in February, males start a permanent spermatophore production and vitellogenic females produce eggs (Cuzin-Roudy, 1993).

Despite a sexual regression in both sexes after the reproductive season (Cuzin-Roudy, 1993), growth did not recover to a high rate, as described for other populations (Ruud, 1936; Einarsson, 1945; Jørgensen and Matthews, 1975; Falk-Petersen and Hopkins, 1981; Mauchline, 1985). The second cohort always represented a significant part of the population. This may result from the accumulation of slow-growing older age classes, as postulated by Berkes (1976) for the populations in the Gulf of Saint Lawrence.

The observed mean size of the 1+ cohort was at maximum 32–33 mm. It is smaller than the 1+ size of *M.norvegica* in the Atlantic Ocean and in the North Sea. Lindley (1982) and Boysen and Buchholz (1984) found a maximal mean size near 35–36 mm, and Falk-Petersen and Hopkins (1981) one greater than 40 mm. Our results are consistent with the values reviewed by Casanova (1981) in a geographical comparison of the maximum size of *M.norvegica*.

The growth rate calculated here for the 0+ cohort ($1.56 \text{ mm month}^{-1}$) corresponds to the highest values given by Boysen and Buchholz (1984) (from 0.4 to 2 mm month^{-1}). It is also closer to the experimental average value of $1.5 \text{ mm month}^{-1}$ obtained under rearing conditions by Fowler *et al.* (1971) on krill from the Ligurian population, with extreme values of 0.96 and $2.5 \text{ mm month}^{-1}$. The k parameter of the von Bertalanffy growth curve fitted to our data (0.0037) falls in the range of 0.0177 – 0.0012 calculated by Matthews (1973) for the 0+ cohort of the Western Norway population.

During the summer months, the first cohort shows a wide size range, indicating that it results from a long spawning period, as already observed by Ruud (1936) for the Mediterranean krill and also by Boysen and Buchholz (1984) for the population of the Kattegat. These results contrast with those for the population of the Clyde which showed two distinct peaks of brood (Mauchline and Fisher, 1969).

Mortality

Mortality is the most difficult function to fit in population dynamics, because its estimation is based on several assumptions that are difficult to verify e.g. (i) the mortality coefficient m is constant for the different age groups, allowing the use of a single exponential mortality model; (ii) the fluctuations in successive recruitments are small and of random character; and (iii) the studied samples represent the average population structure. Concerning invertebrates, the last condition can usually be met by pooling several samples (Brey, 1986). Although mortality variations are known for other populations of *M.norvegica* (Mauchline and Fisher, 1969), we decided here to use a single exponential model for a rough but realistic global estimation of mortality for the Ligurian population.

The average relative proportion calculated for the two modes, 71.4% for the first and 28.6% for the second, and the fitted mortality coefficient, 0.00342 day^{-1} or 1.248 year^{-1} , agree with values extrapolated from Matthews (1973) – average

relative proportion of 75% and 25% for the two modes in January and February, and mortality $0.004-0.01 \text{ day}^{-1}$. The proportions of the 0-group, given by Mauchline (1960), were 66% of the adult population in March and 75–80% in April.

Allen (1971) showed that in a steady-state situation, the coefficient of mortality of a population is equal to the production/biomass (P/B) ratio if the mortality function is a single negative exponential. In our case and under this assumption, the P/B ratio is equal to 1.24 and falls close to the range (from 1.3 to 6.3) given by Lindley (1982) and to the value (1.6) given by Mauchline (1985).

Simulation of the theoretical population

The correspondence between simulated and observed size structures is satisfactory. However, a given size structure can be the result of inverse interactions between growth and mortality functions. The association of a high growth rate and a low mortality rate will increase the relative importance of large size classes. Conversely, a low growth rate and a high mortality rate will increase the relative importance of the small size classes. In the case of the Ligurian population, the stability of the growth pattern from year to year suggests that the results are globally robust.

In conclusion, despite a large instantaneous variability between samples, the demographic parameters of the Ligurian population of *M.norvegica* could be established with precision. The population is characterized by a rapid growth during ~10 months, followed by an almost complete arrest at a size of ~31 mm, which corresponds to the period of reproductive effort for the first year. The average longevity is close to 6.7 months. These characteristics may be viewed as a response to the relatively warm and constant environment (13°C all year round in the Ligurian Sea under the thermocline). They illustrate Bergmann's rule, relating maximal size and latitude, and fit in the latitudinal scheme described by Levinton (1983) among species that maximize their growth rate in a given temperature regime by attaining a smaller maximum body size.

Even in euphausiids that moult throughout their life, an alternation in the life cycle between growth and reproductive periods is a strategy that appears as a necessity to ensure survival in long-lived iteroparous malacostracan crustaceans (Nelson, 1991). Therefore, a high growth rate in summer, reproduction in winter and recruitment in spring, when the primary production is maximum, together with a rather low mortality rate, can be viewed as functional adaptive strategies of *M.norvegica* to the climatic regime of the Ligurian Sea.

References

- Abramson,N.J. (1971) Computer programs for fish stock assessment. *F.A.O. Fish. Tech. Pap.*, **101**, p. 4 + unpag.
Allen,K.R. (1971) Relation between production and biomass. *J. Fish. Res. Board Can.*, **28**, 1573–1581.
Astthorsson,O.S. (1990) Ecology of the euphausiids *Thysanoessa raschi*, *T.inermis* and *Meganyc-
tiphanes norvegica* in Isafjord-deep, northwest-Iceland. *Mar. Biol.*, **107**, 147–157.
Badia,J. and Do-Chi,T. (1976) Etude de la cinétique de la structure des populations de *Squilla mantis*
(Crustacea: Stomatopoda) par l'analyse factorielle des correspondances. *Mar. Biol.*, **36**, 159–169.
Benzecri,J.P. (1973) *L'analyse des données. Tome II-L'analyse des correspondances*. Dunod, Paris, 619 pp.

- Berkes,F. (1976) Ecology of Euphausiids in the Gulf of St. Lawrence. *J. Fish. Res. Board Can.*, **33**, 1894–1905.
- Boucher,J. and Thiriot,A. (1972) Zooplancton et micronecton estivaux des deux cents premiers mètres en Méditerranée Occidentale. *Mar. Biol.*, **15**, 47–56.
- Boucher,J., Ibanez,F. and Prieur,L. (1987) Daily and seasonal variations in the spatial distribution of zooplankton populations in relation to the physical structure in the Ligurian sea front. *J. Mar. Res.*, **45**, 133–173.
- Boysen,E. and Buchholz,F. (1984) *Meganctiphanes norvegica* in the Kattegat. Studies on the annual development of a pelagic population. *Mar. Biol.*, **79**, 195–207.
- Brey,T. (1986) Estimation of annual P/B-ratio and production of marine benthic invertebrates from length-frequency data. *Ophelia*, **4** (Suppl.), 45–54.
- Casanova,J.P. (1981) Nouvelles formulations des règles écologiques connues sous le nom de règle de Bergmann et de loi de Jordan. *J. Plankton Res.*, **3**, 509–529.
- Cuzin-Roudy,J. (1993) Reproductive strategies of the Mediterranean krill, *Meganctiphanes norvegica* and the Antarctic krill, *Euphausia superba* (Crustacea: Euphausiacea). *Invertebr. Reprod. Dev.*, **23**, 105–114.
- de Labigne,C. (1985) Etude du métabolisme nutritionnel et des variations spatio-temporelles de l'environnement trophique potentiel de *Meganctiphanes norvegica* (Euphausiacea) en mer Ligure. Thèse de 3e cycle, Université P. et M.Curie (Paris 6), 137 pp.
- Einarsson,H. (1945) Euphausiacea, I Northern Atlantic species. *Dana Rep.*, **27**, 1–175.
- Falk-Petersen,S. and Hopkins,C.C.E. (1981) Ecological investigations on the zooplankton community of Balsfjorden, northern Norway: population dynamics of the euphausiids *Thysanoessa inermis* (Krøyer), *Thysanoessa raschii* (M.Sars) and *Meganctiphanes norvegica* (M.Sars) in 1976 and 1977. *J. Plankton Res.*, **3**, 177–192.
- Falk-Petersen,S. and Kristensen,A. (1985) Acoustic assessment of krill stocks in Ullsfjorden, North Norway. *Sarsia*, **70**, 83–90.
- Fowler,S.W., Benayoun,G. and Small,L.F. (1971) Experimental studies on feeding, growth and assimilation in a Mediterranean euphausiid. *Thalassia Jugosl.*, **7**, 35–47.
- Franqueville,C. (1970) Etude comparative de macroplancton en Méditerranée nord-occidentale par plongées en soucoupe SP 350, et pêches au chalut pélagique. *Mar. Biol.*, **5**, 172–179.
- Gower,J.C. (1987) Introduction to ordination techniques. In Legendre,P. and Legendre,L. (eds), *Developments in Numerical Ecology*. NATO ASI Ser., **G14**, 3–64.
- Grant,A., Morgan,P.J. and Olive,P.J.W. (1987) Use made in marine ecology of methods for estimating demographic parameters from size/frequency data. *Mar. Biol.*, **95**, 201–208.
- Harding,J.P. (1949) The use of probability paper for the graphical analysis of polymodal frequency distributions. *J. Mar. Biol. Assoc. UK*, **28**, 141–153.
- Hasselblad,V. (1966) Estimation of parameters for a mixture of normal distributions. *Technometrics*, **8**, 431–444.
- Hollingshead,K.W. and Corey,S. (1974) Aspects of life history of *Meganctiphanes norvegica* (M.Sars). Crustacea (Euphausiacea) in Passamaquoddy Bay. *Can. J. Zool.*, **52**, 495–505.
- Ibanez,F. and Boucher,J. (1987) Anisotropie des populations zooplanctoniques dans la zone frontale de mer Ligure. *Oceanol. Acta*, **10**, 205–216.
- Isaacs,J.D. and Kidd,L.W. (1953) Isaacs-Kidd mid-water trawl. *Scripps Inst. Oceanogr. Ref.*, **53**, p. 18.
- Jørgensen,G. and Matthews,J.B.L. (1975) Ecological studies on the deep-water pelagic community of Korsfjorden, Western Norway. *Sarsia*, **59**, 67–84.
- Labat,J.Ph. (1991) Model of a shrimp population (*Philocheras trispinosus*) I. Simulation of the size structure. *Ecol. Model.*, **53**, 75–93.
- Levinton,J.S. (1983) The latitudinal compensation hypothesis: growth data and a model of latitudinal growth differentiation based upon energy budgets. I. Interspecific comparison of Ophryotrocha (Polychaeta: Dorvilleidae). *Biol. Bull.*, **165**, 686–698.
- Lindley,J.A. (1982) Population dynamics and production of Euphausiids. III. *Meganctiphanes norvegica* and *Nyctiphanes couchii* in the North Atlantic Ocean and the North Sea. *Mar. Biol.*, **66**, 37–46.
- Matthews,J.B.L. (1973) Ecological studies on the deep-water pelagic community of Korsfjorden, Western Norway – Population dynamics of *Meganctiphanes norvegica* (Crustacea, Euphausiacea) in 1968 and 1969. *Sarsia*, **54**, 75–90.
- Mauchline,J. (1960) The biology of the euphausiid crustacean, *Meganctiphanes norvegica* (M.Sars). *Proc. Zool. Soc. London*, **132**, 627–639.
- Mauchline,J. (1985) Growth and production of Euphausiacea (Crustacea) in the Rockall Trough. *Mar. Biol.*, **90**, 19–26.
- Mauchline,J. and Fisher,L.R. (1969) The biology of euphausiids. *Adv. Mar. Biol.*, **7**, 1–454.

- Miquel, J.C. and Labat, J.Ph. (1992) Distribution of crustacean micronekton across a mediterranean front. *Rapp. Comm. Int. Mer Médit.*, **33**, 261.
- Nelson, K. (1991) Scheduling of reproduction in relation to molting and growth in malacostracan crustaceans. In Wenner, A. and Kuris, A. (eds), *Crustacean Issues*. Balkema, Rotterdam, Vol. 7, pp. 77–113.
- Nicol, S. (1986) Shape, size and density of daytime surface swarms of the euphausiid *Meganyctiphanes norvegica* in the Bay of Fundy. *J. Plankton Res.*, **8**, 29–39.
- Omori, M. (1965) A 160-cm opening-closing plankton net. *J. Oceanogr. Soc. Jpn.*, **21**, 20–26.
- Orsi Relini, L. (1992) The fin whale and other pelagic filterers as samplers of *Meganyctiphanes norvegica*. *Rapp. Comm. Int. Mer Méditerr.*, **33**, 263.
- Orsi Relini, L. and Relini, G. (1993) *Meganyctiphanes norvegica* nelle reti trofiche del Mar Ligure. *Biol. Mar. Suppl. Not. SIBM*, **1**, 151–154.
- Pearcy, W.G., Hopkins, C.C.E., Grönvik, S. and Evans, R.A. (1979) Feeding habits of cod, capelin, and herring in Balsfjord, northern Norway, July–August 1978: the importance of euphausiids. *Sarsia*, **67**, 269–277.
- Picard, A. (1982) Détermination par l'analyse factorielle de la période approchée d'un phénomène quasi cyclique. Application au développement synchrone des larves portées par une population de vers marins *Spirorbis spirorbis*. *Cah. Anal. Données*, **7**, 290–310.
- Quynh, V.D. (1978) Ecologie des crustacés micronectoniques dans l'écosystème superficiel du bassin liguro-provençal: étude particulière des Décapodes Natantia pélagiques. Thèse de 3e cycle, Université P. et M. Curie (Paris 6), 125 pp.
- Ruud, J.T. (1936) Euphausiacea. *Rep. Dan. Oceanogr. Exped. Mediterr.*, **2**, 1–86.
- Sameoto, D.D. (1983) Euphausiid distribution in acoustic scattering layers and its significance to surface swarms. *J. Plankton Res.*, **5**, 129–143.
- Sanchez, P. (1982) Régimen alimentario de *Illex coindetti* en el mar Catalan. *Invest. Pesq.*, **46**, 443–449.
- Siegel, S. and Castellan, N.J., Jr (1988) *Nonparametric Statistics for Behavioral Sciences*. McGraw-Hill, New York, 399 pp.
- Sokal, R.R. and Rohlf, F.F. (1981) *Biometry*. W.H. Freeman & Co., New York, 859 pp.
- Sournia, A., Brylinski, J.M., Dallot, S., Le Corre, P., Leveau, M., Prieur, L. and Froget, C. (1990) Fronts hydrologiques au large des côtes françaises: Les sites-ateliers du programme Frontal. *Oceanol. Acta*, **13**, 413–438.
- Viale, D. (1985) Cetaceans in the Northwestern Mediterranean: their place in the ecosystem. *Oceanogr. Mar. Biol. Annu. Rev.*, **23**, 491–571.
- Wannacott, T.H. and Wannacott, R.J. (1991) *Statistique*. Economica, Paris, 919 pp.
- Wiebe, P.H. and D'Abramo, L. (1972) Distribution of euphausiid assemblages in the Mediterranean Sea. *Mar. Biol.*, **15**, 139–149.

Received on September 28, 1995; accepted on July 19, 1996